Ceramics International xxx (xxxx) xxx–xxx

Contents lists available at ScienceDirect

Ceramics International

journal homepage: www.elsevier.com/locate/ceramint

Multiferroic properties of $Bi_{0.89}Ho_{0.08}Sr_{0.03}Fe_{0.97-x}Mn_{0.03}Ni_xO_3$ thin films modulated by F–N tunneling effects

Meiyou Guo[a], Guoqiang Tan[a,*], Wei Yang[a], Yun Liu[a], Huijun Ren[b], Ao Xia[a], Long Lv[c], Mintao Xue[a]

[a] School of Materials Science and Engineering, Shaanxi University of Science & Technology, Xi'an 710021, China
[b] School of Arts and Sciences, Shaanxi University of Science & Technology, Xi'an 710021, China
[c] Department of Information Engineering, Engineering University of PAP, Xi'an 710086, China

ARTICLE INFO

Keywords:
$BiFeO_3$ thin film
Co-doping
Fowler–Nordheim tunneling effect
Multiferroic properties

ABSTRACT

$Bi_{0.89}Ho_{0.08}Sr_{0.03}Fe_{0.97-x}Mn_{0.03}Ni_xO_3$ (BHSFMNi$_x$O) films were prepared via a chemical solution deposition method. X-ray diffraction (XRD) patterns and Raman spectroscopy revealed that BHSFMNi$_x$O films showed (100) preferential orientation and the structural transition. The structure of BHSFMNi$_{0.02}$O was close to the morphotropic phase boundary (MPB) (*R3c:H:R3m:R* = 1:1). The oxygen vacancies were increased with an increase in Ni^{2+} doping, and there were many defect dipoles. The BHSFMNi$_x$O thin films exhibited an Ohmic or a space-charge-limited conduction (SCLC) mechanism in a low electric field, and the interface-limited Fowler–Nordheim (F–N) tunneling or the trap-assisted F–N tunneling in a high electric field. The interface-limited F–N tunneling effects of BHSFMNi$_{0.01}$O and BHSFMNi$_{0.02}$O were due to an interface effect. The large remnant polarizations of BHSFMNi$_{0.01}$O and BHSFMNi$_{0.02}$O contributed to the intrinsic polarization and the interface-limited F–N tunneling. The fake polarizations of BHSFMNi$_{0.03}$O and BHSFMNi$_{0.04}$O were dominated by the trap-assisted F–N tunneling in which the interface traps helped the carrier tunnel the potential barrier. These results demonstrate that the polarizations of BHSFMNi$_x$O are related not only to the structural transformation, but also to the defects and conduction mechanisms.

1. Introduction

Among many multiferroic materials, $BiFeO_3$ (BFO) is a unique single-phase multiferric material, whose ferroelectric Curie temperature (T_C = 829.85 °C) and antiferromagnetic order temperature (Neel temperature, T_N = 369.85 °C) are above room temperature [1,2]. BFO has potential applications in many fields, such as nonvolatile ferroelectric random access memories, magnetoelectric storage and spintronic devices, due to the coexistence of ferroelectric (FE) and ferromagnetism (FM). Thus, BFO materials have drawn much attention over the past decade [3]. However, owing to the existence of a large number of charge defects caused by the volatilization of bismuth and the transformation from Fe^{3+} to Fe^{2+}, BFO thin films have suffered from the serious current leakage problems, making it difficult to obtain a saturated electric hysteresis loop. Therefore, the potential applications of BFO thin films in devices were greatly limited [4,5]. The most common approach to improving the multiferroic properties of BFO films was ion substitution. Ion substitution at either Bi or Fe or both sites could influence the structure of BFO films, which could modify the multiferroic properties by changing the defects in BFO films [6,7].

Different doping ions and doping concentrations could influence the orientation of BFO films [8,9]. The different orientations of BFO films had different functions on the multiferroic properties. A (111)-oriented BFO film exhibited giant ferroelectric remnant polarization ($2P_r$ = 196.9 μC/cm^2), while a (100)-oriented BFO thin film possessed a low coercive field ($2E_c$ = 385.5 kV/cm) and almost fatigue-free behavior [10,11]. In addition, morphotropic phase boundary (MPB) behavior could conveniently improve the multiferroic properties of BFO films and could be comprehensively described by the ionic radius at average Fe and Bi sites as a critical parameter, which indicated that the chemical pressure effect caused by substitution was the principle cause of the MPB behavior [12]. A reversible phase transition led to an enhanced piezoelectric response in Sm-doped BFO thin film with MPB composition [13]. Ion doping not only distorted the structure of BFO films, but also affected their defects, for instance, oxygen vacancies. These defects directly affected the leakage current and ferroelectric properties of BFO thin films [14]. The lower concentration of oxygen vacancies resulted in a lower density of free carriers, which could

* Corresponding author.
E-mail address: tan3114@163.com (G. Tan).

https://doi.org/10.1016/j.ceramint.2018.04.015
Received 8 February 2018; Received in revised form 30 March 2018; Accepted 3 April 2018

enhance the insulation of BFO films. The Schottky Barrier Height (SBH) at the interface could be changed in the transmission process of higher levels of oxygen vacancies, which changed the conduction mechanism of the leakage current in BFO films [15,16]. The modulation of the interface barrier for metals and BFO films was significant in the design of BFO semiconductor devices. Obtaining stable Ohmic contact at the interface was beneficial to the characterization of the intrinsic electrical properties. On the other hand, the carrier transportation in BFO films was changed by adjusting the SBH, and then the BFO thin films could obtain better rectifying characteristics. At present, there is a lot of research on the effects of oxygen vacancies on the leakage current density and conduction mechanism. However, it is not clear that what influences the leakage current has on ferroelectric properties in BFO thin films.

In this work, $Bi_{0.89}Ho_{0.08}Sr_{0.03}Fe_{0.97-x}Mn_{0.03}Ni_xO_3$ (x = 0.01–0.04) thin films were prepared using the chemical solution deposition (CSD) method. The different conduction mechanisms of leakage current caused by the transport and distribution of oxygen vacancies in the inside and the interface of BFO films were investigated. The influences of different Fowler–Nordheim (F–N) tunneling effects on the ferroelectric properties of BFO thin films were discussed, and the relationship between the leakage current conduction mechanisms of BFO films and ferroelectric properties was studied.

2. Experimental procedure

$Bi_{0.89}Ho_{0.08}Sr_{0.03}Fe_{0.97-x}Mn_{0.03}Ni_xO_3$ (x = 0.01–0.04) thin films were prepared on FTO/glass substrates (FTO is a fluorine-doped tin oxide conductive film) by the CSD method. The precursor solutions were prepared using $Bi(NO_3)_3{\cdot}5H_2O$, $Sr(NO_3)_2$, $Ho(NO_3)_3{\cdot}6H_2O$, $Fe(NO_3)_3{\cdot}9H_2O$, $C_4H_6NiO_4{\cdot}4H_2O$ and $C_4H_6MnO_4{\cdot}4H_2O$ as raw materials, which were then mixed together in an atomic ratio of $0.94{:}0.08{:}0.03{:}0.97-x{:}0.03{:}x$ (x = 0.01, 0.02, 0.03, 0.04) (5 mol% of excess Bi was added to compensate for bismuth loss during the heat treatment). The raw materials were dissolved in acetic anhydride and 2-methoxyethanol solvents based on the solution concentration (0.3 mol/L) and the volume ratio of acetic anhydride and 2-methoxyethanol was 1:3. To obtain the homogeneous precursor solutions, the solutions were stirred continuously for 120 min at room temperature. The precursor solution was spin-coated on FTO glass, and the speed and the time of rotation were 4000 rpm and 15 s, respectively. After spin-coating, volatile materials were immediately removed from the wet films at 200 °C for 10 min, and the films were annealed in air at 550 °C for 10 min. In order to obtain a suitable thickness of BFO film, the above processes were repeated 13 times. Top Au electrodes with areas of 0.003 mm^2 were prepared through a mask on the surface of the BFO film by ion sputtering. After annealing at 285 °C for 30 min, the Au electrodes were in complete contact with the films.

The structures of the thin films were studied by an X-ray diffraction (XRD, Rigaku, D/MAX-2200) using Cu Kα radiation (0.15418 nm). Raman spectra were obtained by a micro Raman spectrometer with an Ar ion laser excitation at 532 nm. An X-ray photoelectron spectroscopy (XPS, XSAM800) was used to study the valence states of the ions of the BFO thin films [17]. The leakage current densities of the BFO thin films were tested by an Agilent B2901A instrument. Capacitance–voltage (C–V) measurements were carried out with an Agilent E4980A Concise LCR meter. The hysteresis loops of the thin films were tested by a Radiant Multiferroic system. At room temperature the ferromagnetic properties of the thin films were analyzed using a superconducting quantum interference magnetic measuring system (MPMS-XL-7).

3. Results and discussion

Fig. 1(a) shows the XRD patterns of the $Bi_{0.89}Ho_{0.08}Sr_{0.03}Fe_{0.97-x}Mn_{0.03}Ni_xO_3$ (BHSFMNi_xO) thin films. The BHSFMNi_xO thin films are indexed for their distorted rhombohedral structure on Standard PDF Card (JCPDS No. 74-2016). No impurity phase is detected in any of the BHSFMNi_xO thin films. With an increase in Ni^{2+} doping, the ratios of the intensity of the (100) diffraction peak to (1–10) in the BHSFMNi_xO (x = 0.01, 0.02, 0.03 and 0.04) films are 2.234, 2.334, 1.094 and 1.211 in turn, which shows that all the BHSFMNi_xO thin films are polycrystalline BFO phases with a (100) preferential orientation, especially in BHSFMN$i_{0.01}$O and BHSFMN$i_{0.02}$O thin films. While most of the BFO-based films on FTO substrates have an obvious (110) preferential orientation [18,19], which means that Ni^{2+} doping leads to the structural transformation. Rietveld refinement of the XRD patterns is performed to further analyze the effects of Ni^{2+} doping on the structures of BHSFMNi_xO films, and the refinement results are shown in Fig. 1(b) and Table 1. The error factors (Rw) are below 11%, which indicates that the refinement results are consistent with the experimental data. According to the refinement results, BHSFMNi_xO thin films show the state of two-phase coexistence,

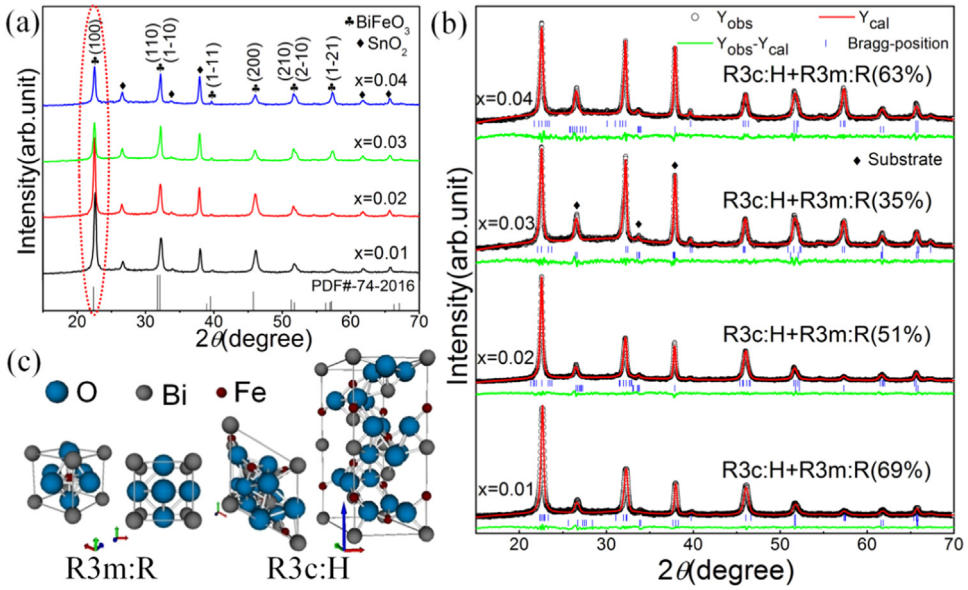

Fig. 1. (a) XRD patterns of $Bi_{0.89}Ho_{0.08}Sr_{0.03}Fe_{0.97-x}Mn_{0.03}Ni_xO_3$ (BHSFMNi_xO, x = 0.01–0.04) thin films; (b) Rietveld-refined XRD patterns of BHSFMNi_xO thin films; (c) structural models of *R3m:R* and *R3c:H* space groups.